Concentration-Dependent Interactions of the Organophosphates Chlorpyrifos Oxon and Methyl Paraoxon with Human Recombinant Acetylcholinesterase

R. Kaushik[*], **Clint A. Rosenfeld**[†], and **L.G. Sultatos**[*],[1]

[*] *Department of Pharmacology and Physiology, University of Medicine and Dentistry of New Jersey, New Jersey Medical School, Newark, New Jersey 07103*

[†] *Drug Metabolism and Pharmacokinetics, Schering-Plough Research Institute, Lafayette, New Jersey 07843*

Abstract

For many decades it has been thought that oxygen analogs (oxons) of organophosphorus insecticides phosphylate the catalytic site of acetylcholinesterase by a mechanism that follows simple Michaelis-Menten kinetics. More recently, the interactions of at least some oxons have been shown to be far more complex, and likely involve binding of oxons to a second site on acetylcholinesterase that modulates the inhibitory capacity of other oxon molecules at the catalytic site. The current study has investigated the interactions of chlorpyrifos oxon and methyl paraoxon with human recombinant acetylcholinesterase. Both chlorpyrifos oxon and methyl paraoxon were found to have k_i's that change as a function of oxon concentration. Furthermore, 10 nM chlorpyrifos oxon resulted in a transient increase in acetylthiocholine hydrolysis, followed by inhibition. Moreover, in the presence of 100 nM chlorpyrifos oxon, acetylthiocholine was found to influence both the K_d (binding affinity) and k_2 (phosphorylation constant) of this oxon. Collectively, these results demonstrate that the interactions of chlorpyrifos oxon and methyl paraoxon with acetylcholinesterase cannot be described by simple Michaelis-Menten kinetics, but instead support the hypothesis that these oxons bind to a secondary site on acetylcholinesterase, leading to activation/inhibition of the catalytic site, depending on the nature of the substrate and inhibitor. Additionally, these data raise questions regarding the adequacy of estimating risk of low levels of insecticide exposure from direct extrapolation of insecticide dose-response curves since the capacity of individual oxon molecules at low oxon levels could be greater than individual oxon molecules *in vivo* associated with the dose response curve.

Keywords

organophosphorus insecticides; chlorpyrifos oxon; methyl paraoxon; acetylcholinesterase

Introduction

The interactions of acetylcholinesterase (EC 3.1.1.7) with acetylcholine and the surrogate substrate acetylthiocholine are complex, and have been shown to involve binding of substrate

to the catalytic site as well as a secondary binding site known as the peripheral anionic site (Taylor and Radić, 1994, and Bourne *et al*, 2003). The catalytic triad (Ser-203, His-447, and Glu-334)(all numbers refer to the amino acid position of human acetylcholinesterase) has been shown to be located at the base of an active site gorge, with the peripheral anionic site on the rim of this gorge, including residues Tyr-72, Tyr-124, Trp-286, Tyr-341, and Asp-74 (Sussman *et al*, 1991; Barak *et al*, 1995; and Bourne *et al*, 2003). Interestingly, these two sites have been described as working in tandem, where occupation of the peripheral anionic site can decrease or increase activity at the catalytic site (Johnson *et al*, 2003). For example, at high concentrations both acetylcholine and acetylthiocholine have been shown to bind to the peripheral anionic site, leading to substrate inhibition as a result of reduced substrate hydrolysis through steric blockade and/or conformation changes in Trp-86 and Tyr-133 residues within the active site gorge (Taylor and Radić, 1994; Barak *et al*, 1995; and Bourne *et al*, 2003). Conversely, Szegletes *et al* 1999 have reported that cationic substrates can form a low affinity complex at the peripheral anionic site that accelerates hydrolysis at low substrate concentrations, but results in substrate inhibition at high concentrations (Mallender *et al*, 2000). Occupation of the peripheral anionic site of *Drosophila* acetylcholinesterase by D-tubocurarine has been shown to increase methanesulfonylation of the active site (Golicnik *et al*, 2002), whereas occupation of the peripheral anionic site of *Drosophila* acetylcholinesterase by Triton X-100 has been reported to increase and decrease inhibition brought about by certain organophosphates and carbamates (Marcel *et al*, 2000).

Given the obvious complexities involved in the interactions of acetylcholinesterase with various substrates and peripheral anionic site ligands, it should not be surprising that the inhibition of acetylcholinesterase by the active metabolites (called oxons or oxygen analogs) of at least some organophosphorus insecticides is not as simple as was originally thought. For many decades it was believed that oxons phosphylated Ser-203 of the active site, according to the simplest scheme in Figure 1.

Based on this scheme, Main (1964) introduced the inhibitory constant k_i, which is defined as follows:

$$k_i = k_2 / K_d \qquad \text{Equation (1)}$$

where

$$K_d = k_{-1} / k_1 \qquad \text{Equation (2)}$$

The rate constants k_1, k_{-1}, and k_2 are the same as those shown in Figure 1. With this scheme, the value of k_i is specific for each oxon, and correlates directly with the inhibitory capacity of an oxon. Additionally, this scheme dictates that a k_i must be of constant value for any particular oxon. However, more recent studies have reported that under certain conditions, the k_is of certain oxons change as a function of the oxon concentrations, indicating that the inhibitory capacities of these oxons change as a function of oxon concentration (Kardos and Sultatos, 2000,Kousba *et al*, 2004, and Rosenfeld and Sultatos, 2006). These reports have suggested that certain oxons might also reversibly bind to a secondary site on acetylcholinesterase, thereby reducing the capacity of additional oxon molecules from interacting with the active site, although it must be noted that no evidence has yet been presented that they bind to the peripheral anionic site.

The characterization of those factors that affect the capacity of oxons to inhibit acetylcholinesterase is an important step in understanding the risks posed to public health by organophosphorus insecticides since cholinergic crisis observed after exposure to these chemicals is mediated through inhibition of acetylcholinesterase (Mileson *et al*, 1998). The

current report investigates concentration-dependent interactions of human recombinant acetylcholinesterase with chlorpyrifos oxon and methyl paraoxon, and investigates how the presence of substrate might influence the capacity of chlorpyrifos oxon to inhibit this important enzyme.

Materials and Methods

Chemicals

Chlorpyrifos oxon (*O*,*O*–diethyl *O*–(3,5,6-trichloro-2-pyridyl) phosphate) and methyl paraoxon (*OO*, -dimethyl *O*-(4-nitrophenyl) phosphate) were purchased from Chem Services (West Chester, PA). Human recombinant acetylcholinesterase, bovine serum albumin, and all other chemicals used were purchased from Sigma Chemical Company (St. Louis, MO).

Determination of k_i by the k_i model

Except where noted, each k_i was determined as described by Rosenfeld and Sultatos (2006). All studies were done with 100 mM sodium phosphate buffer (pH 7.4) containing bovine serum albumin at a concentration of 1 mg/ml (Rosenfeld and Sultatos, 2006). With this approach, acetylcholinesterase was incubated with a specified concentration of inhibitor for specified periods of time. At each indicated time the reaction was stopped by dilution with a large volume containing 0.44 mM acetylthiocholine, and the Ellman reaction (Ellman *et al*, 1961) was monitored at 405 nm in a plate reader (BIO-TEK Instruments., Winoski, VT) in order to quantify uninhibited acetylcholinesterase activity (see Rosenfeld and Sultatos, 2006 for details of this methodology). The empirical data (uninhibited acetylcholinesterase active site concentration over time) were fitted with the software ACSL (Advanced Continuous Simulation Language, Aegis, Huntsville, AL) to the following equations, which were slightly modified from Rosenfeld and Sultatos (2006) in order to reflect the spontaneous breakdown of chlorpyrifos oxon and methyl paraoxon:

$$d[\mathrm{EA}]/dt = k_i * [\mathrm{E}] * [\mathrm{AB}] - k_3 * [\mathrm{EA}] - k_4 * [\mathrm{EA}] \qquad \text{Equation (3)}$$

$$d[\mathrm{EA_{Age}}]/dt = k_4 * [\mathrm{EA}] \qquad \text{Equation (4)}$$

$$d[\mathrm{AB}]_{Sp}/dt = k_5 * [\mathrm{AB}] \qquad \text{Equation (5)}$$

$$[\mathrm{E}] = [\mathrm{E_T}] - [\mathrm{EA}] - [\mathrm{EA_{Age}}] \qquad \text{Equation (6)}$$

$$[\mathrm{AB}] = [\mathrm{AB_T}] - [\mathrm{B}] - [\mathrm{AB_{Sp}}] \qquad \text{Equation (7)}$$

As shown by Rosenfeld and Sultatos (2006), E_T represents the initial active site concentration (determined as described by Rosenfeld and Sultatos, 2006), while AB_T represents the initial chlorpyrifos oxon or methyl paraoxon concentrations. In addition k_5 represents the first order rate constant for spontaneous decomposition of chlorpyrifos oxon or methyl paraoxon, and $[AB_{Sp}]$ represents the concentration of oxon that has undergone spontaneous (non-enzymatic) decomposition. All other parameters used in equations 3–7 have the same meaning as those in Figure 1. The rate constants for activation (k_3) and aging (k_4) were taken from the literature, and were 0.005379 h^{-1} and 0.001575 h^{-1}, respectively, for chlorpyrifos oxon (Masson *et al*, 2000), and 0.7 h^{-1} and 3.7 h^{-1}, respectively, for methyl paraoxon (Worek *et al*, 2000). Some k_is were also calculated by the traditional method of Main (1964), as described by Rosenfeld and Sultatos (2006).

Determination of the K_d and k_2 for chlorpyrifos oxon

The determinations of K_d and k_2 were accomplished by a technique termed the zero-time method (Gray and Duggleby, 1989), originally developed by Hart and O'Brien (1973). As described by Gray and Duggleby (1989), this approach determines these kinetic parameters by monitoring the hydrolysis of a single substrate (acetylthiocholine) concentration in the absence and presence of a single concentration of inhibitor (chlorpyrifos oxon). The K_d is determined from the following equation:

$$K_d = (K_m * [\text{inhibitor}]) / ((K_m + [\text{substrate}]) * (v_c / v_o - 1))$$

Equation (8)

Where v_c is the control velocity (absence of inhibitor) and v_o is the initial velocity in the presence of inhibitor. The v_o was determined by first fitting thiocholine production with time to:

$$[\text{P}] = [\text{P}]_\infty * (1 - e^{-A*[\text{inhibitor}]*t})$$

Equation (9)

where [P] and $[\text{P}]_\infty$ are concentrations of product (thiocholine) at any time t, and at t = ∞, respectively (Liu and Tsou, 1986, and Gray and Duggleby, 1989). The constant "A" represents the apparent rate constant for the formation of inhibited enzyme. The continually changing slopes of this progressive inhibition curve were obtained by cubic spline analysis of the fitted curve from Equation (9)(Barak *et al*, 1995). As described by Hart and O'Brien (1973), and Barak *et al* 1995, semilogarithmic plots of these slopes against time yielded straight lines, where the intercepts equal v_o in Equation (8).

The K_m for the breakdown of acetylthiocholine by acetylcholinesterase was determined as previously described (Rosenfeld *et al*, 2001) with the Haldane equation, since acetylthiocholine is known to display substrate inhibition (Radić *et al*, 1993). For K_m determinations, hydrolysis of acetylthiocholine at 37° was followed in the presence of 0.1 mM 5,5′-dithio-*bis*(2-nitrobenzoic acid)(DTNB) in a Shimadzu MPS 2000 UV-Vis spectrophotometer (Shimadzu Scientific Instruments, Inc., Columbia, MD), set at a wavelength of 412 for acetylthiocholine. All co-incubations of chlorpyrifos oxon and acetylthiocholine were carried out at 24° or 37° in a SX20 stopped-flow spectophotometer (Applied Photophysics Limited, Leatherhead, United Kingdom). The instrument had a 20 μl flow cell with the light path set to 10 mm. The wavelength was set to 412 nm, with monochromator slit width openings of 5 mm. All solutions were prepared in 100 mM sodium phosphate buffer (pH 7.4) containing 1mg/ml bovine serum albumin (Rosenfeld and Sultatos, 2006). DTNB, which was included with the indicated acetylthiocholine concentrations, was added to give a final concentration in the flow cell of 1 mM. The concentrations of acetylthiocholine were selected so as not to exceed the K_m of this substrate, thereby maintaining pseudo first order conditions (Hart and O'Brien, 1973). Additionally, hydrolysis of acetylthiocholine over time in all control incubations was linear.

Following determination of K_d, k_2 was calculated from:

$$k_2 = (\Delta(\ln_v)/\Delta t) * (K_d/([\text{inhibitor}] * (1 - \alpha)) + 1)$$

Equation (10)

where $\Delta(\ln_v)/\Delta t$ is the slope obtained from the semilogarithmic plot of the continually changing slopes of the progressive inhibition curve (Hart and O'Brien, 1973, and Barak *et al*, 1995), and where:

$$\alpha = [\text{substrate}]/(K_m + [\text{substrate}])$$

Equation (11)

Modeling and statistical analyses

All modeling studies for k_i were carried out on a laptop or desktop computer using ACSL 11.8 (Advanced Continuous Simulation Language Aegis, Huntsville, AL). Statistical analyses and regression analyses were carried out with Sigmastat and Sigmaplot (SPSS Science Inc., Chicago, IL).

Results

Chlorpyrifos oxon or methyl paraoxon in buffer were incubated at 24° or 37° in the absence of enzyme for varying lengths of time. The chlorpyrifos oxon and methyl paraoxon levels were monitored by quantifying the capacity of a sample of the incubation to inhibit human recombinant acetylcholinesterase. Both oxons underwent non-enzymatic breakdown, as evidenced by the reduction in inhibitory capacity of samples from the incubations (Figure 2). These rates of breakdown could be described by first order rate constants (Figure 2), which were incorporated into the k_i model in order to account for all oxon during incubations in the presence of enzyme.

Incubation of human recombinant acetylcholinesterase with different concentrations of chlorpyrifos oxon or methyl paraoxon at 24° or 37° for various periods of time gave inhibition profiles that could be optimized with the k_i model in order to determine the k_i for each oxon (see Figure 3 for representative examples). A temperature of 24° was used because many previous k_i determinations have been done at this temperature, while 37° was utilized because of its physiological significance. When the k_is were determined in this manner with oxon concentrations ranging from about 2nM – 100 nM, it was found that the k_i for each oxon varied as a function of oxon concentration (Figures 3 and 4). Note that a larger k_i corresponds to a greater capacity to inhibit acetylcholinesterase. With both chlorpyrifos oxon and methyl paraoxon, at both 24° and 37°, the relationship between oxon concentration and k_i was described by a rectangular hyberbola. The asymptotes obtained at the higher oxon concentrations corresponded well with the k_is calculated by the traditional method of Main (1964)(Rosenfeld and Sultatos, 2006)(Figures 4 and 5).

As described by Gray and Duggleby (1989), the zero-time method can be used to determine the K_d and k_2 of an oxon towards acetylcholinesterase with a profile of acetylthiocholine hydrolysis at a single substrate and single inhibitor concentration (Hart and O'Brien, 1973). This approach requires knowledge of the K_m for hydrolysis of acetylthiocholine by acetylcholinesterase (Equation 8), which was determined to be 0.1044 mM at 37° (Figure 6). The substrate inhibition observed at the higher concentrations of acetylthiocholine (Figure 6) has been previously reported, and involves binding of this surrogate substrate to the peripheral anionic site of acetylcholinesterase (Radić *et al*, 1993).

Hydrolysis of three different concentrations of acetylthiocholine in the presence of 100 nM chlorpyrifos oxon was quantified by stopped-flow spectrophotometry in order to minimize the error associated with the zero-time method (Gray and Duggleby, 1989). Figure 7 shows the product profiles with time, as well as the secondary plots from which the intercepts and slopes were taken for equations 8 and 10. Surprisingly, the *appK$_d$*, *appk$_2$*, and *appk$_i$* for chlorpyrifos oxon changed as a function of the acetylthiocholine concentration (Fig. 8). The lowest acetylthiocholine concentration utilized (0.01375 mM) yielded the highest *appK$_d$*, *appk$_2$*, and the lowest *appk$_i$* (Figure 8). With an acetylthiocholine concentration of 0.01375 mM, addition of 10 nM chlorpyrifos oxon unexpectedly, transiently elevated the velocity of acetylthiocholine hydrolysis (Figure 9). In this regard, for a period of time (51–81 s) following initiation of the incubation, acetylthiocholine hydrolysis rates in the presence of 10 nM chlorpyrifos oxon exceeded that of controls (without chlorpyrifos oxon)(Figure 9). This enhanced activity was

reflected in the greater initial velocity, determined from the y intercepts in the lower panel of Figure 9, in the presence of 10 nM chlorpyrifos oxon (Figure 10).

Discussion

Two observations in the present report document that chlorpyrifos oxon and methyl paraoxon cannot interact with acetylcholinesterase in a manner consistent with the simple Michaelis-Menten kinetics on which the k_i model was derived (Main, 1964). The first is the changing k_is as a function of oxon concentration (Figures 4 and 5). An accurate description of the interactions of these oxons with acetylcholinesterase must include a mechanism whereby oxon molecules reduce the capacity of other, subsequent oxon molecules to inhibit the catalytic site. The second observation demonstrating non-Michaelis-Menten kinetics is the acceleration of acetythiocholine hydrolysis followed by inhibition, resulting from 10 nM chlorpyrifos oxon (Figures 9 and 10). The inhibition obviously reflects the phosphorylation of Ser-203. However, early within the incubation, before significant phosphorylation has occurred, the accelerated hydrolysis of acetylthiocholine had to result from some presently unknown interaction of chlorpyrifos oxon and enzyme separate from the phosphorylation event.

Complex kinetics have been documented for many substrates and inhibitors of acetylcholinesterase, probably as a result of interactions between the peripheral anionic and catalytic sites. For example, Johnson *et al* 2003 have proposed that the peripheral anionic site, which is located at the rim of the active site gorge (Bourne *et al* (2003) transiently binds substrate for human acetylcholinesterase on the way to the catalytic site. Their modeling studies have suggested that the peripheral anionic site can accelerate events at the catalytic site with certain substrates/ligands at low concentrations, while inhibiting those same events at high ligand concentrations, perhaps due to the blockage of product dissociation from the catalytic site (Mallender *et al*, 2000, and Johnson *et al*, 2003). Similarly, Stojan *et al* 1998, using *Drosophila* melanogaster acetylcholinesterase, have proposed that initial binding to the peripheral anionic site increases the probability of a molecule entering the active site gorge, while continued occupation of the peripheral anionic site decreases the rate of entrance of subsequent molecules into the active site gorge. In addition they have proposed that occupation of the catalytic site lowers the affinity of the peripheral anionic site for substrate (Stojan *et al*, 1998). Thus their model was able to account for apparent enzyme activation at low substrate concentration, and enzyme inhibition at high substrate concentration (Stojan *et al*, 1998). Likewise, Masson *et al* 2000 have proposed that substrate inhibition and activation of acetylcholinesterase are linked features of a common allosteric conformational process triggered by substrate binding to the peripheral anionic site. Given the similarities in the actions of chlorpyrifos oxon and methyl paraoxon in modulating their own inhibitory capacities (Figures 4 and 5) to those of previously reported substrates/ligands for acetylcholinesterase (see above discussion), it seems likely that these oxons are binding to a secondary site on acetylcholinesterase separate from the catalytic site (Figure 1), as was suggested in previous studies (Kardos and Sultatos, 2000; Kousba *et al*, 2005; and Rosenfeld and Sultatos, 2006). However, it must be noted that such a putative site has not yet been identified for these oxons.

Co-incubation of three different concentrations of acetylthiocholine with 10 nM chlorpyrifos oxon and acetylcholinesterase revealed that acetylthiocholine can alter the inhibitory capacity of chlorpyrifos oxon (Figure 8). Increasing the acetylthiocholine concentration from 0.01375 mM to 0.0275 mM appeared to increase the binding affinity of chlorpyrifos oxon (as evidenced by a decreased K_d), yet reduce the oxon's capacity to phosphorylate Ser-203 (as evidenced by a reduced k_2)(Figure 8). The net effect of these alterations was to increase k_i, the inhibitory capacity, by about 59 % (Figure 8). Other peripheral site ligands such as propidium, gallamine, and d-tubocurarine, have been preiously reported to accelerate the inhibition of recombinant mouse acetylcholinesterase by paraoxon and other neutral organophosphates (Radić and

Taylor, 1999, and Radić and Taylor, 2001). Radić and Taylor (2001) concluded that ligands binding to the peripheral anionic site altered the conformation of those amino acids lining the choline binding site, thereby providing a more efficient fit of the leaving groups of uncharged organophosphates. Since acetylthiocholine (as well as acetylcholine) is also a peripheral site ligand, one can reasonably conclude a similar action towards chlorpyrifos oxon in the current study, particularly in view of the observed reduction in K_d brought by acetylthiocholine (Figure 8). Additionally, the current report demonstrated an effect on k_2 also resulting from acetylthiocholine (Figure 8). However, it must be remembered that the actions of acetylthiocholine documented in Figure 8 are occurring in the presence of 100 nM chlorpyrifos oxon, which by itself caused a striking reduction in its own k_i (Figure 4). It should be noted that physiological concentrations of acetylcholine, although highly variable, have been reported to reach the millimolar range in narrow synaptic clefts following evoked release (Van Der Kloot and Molg (1994). Consequently, transient occupation of the peripheral anionic site by acetylcholine *in vivo* likely occurs.

Although the details of the interactions of these oxons with acetylcholinesterase other than the phosphorylation of Ser-203 are not known with certainty at the present time, the non-Michaelis-Menten kinetics documented in the current report and elsewhere (Kardos and Sultatos, 2000; Kousba *et al*, 2005; and Rosenfeld and Sultatos, 2006) could have possible implications for the risk assessment of chlorpyrifos and related insecticides. When addressing this issue, however, the relationship between oxon levels that might exist *in vivo* following exposure to insecticides, versus the oxon concentrations that are associated with a changing k_i *in vitro* should be considered. Due to the enormous difficulties in quantification of oxon levels *in vivo* following exposure to organophosphorus insecticides, only one study has systematically provided adequate pharmacokinetic information describing the blood levels of parent insecticide (chlorpyrifos) and corresponding oxon (chlorpyrifos oxon). Timchalk *et al* 2002, utilizing GC-Mass Spec to measure chlorpyrifos oxon concentrations in the rat following oral administration of chlorpyrifos, found that 10 mg/kg chlorpyrifos produced very slight inhibition of brain acetylcholinesterase, with corresponding blood oxon levels of 2–7 nM. Consequently, at least in the rat, dose response curves generated with measurable brain acetylcholinesterase inhibition represent inhibition occurring at chlorpyrifos oxon blood levels higher than 2–7 nM. As shown in Figure 4, with human recombinant acetylcholinesterase the chlorpyrifos oxon k_i is markedly reduced at oxon concentrations higher than about 10 nM. Therefore, extrapolation of such a dose response curve to low insecticide levels could result in an under-estimation of insecticide risk because the capacity of individual chlorpyrifos oxon molecules to inhibit acetylcholinesterase at very low oxon levels could be greater than those individual oxon molecules *in vivo* associated with the dose response curve. Thus, concentration-dependent interactions of certain oxons with acetylcholinesterase might contribute, along with toxicokinetic factors and factors linking acetylcholinesterase inhibition with cholinergic dysfunction, to non-linear dose response relationships.

Bibliography

Barak D, Ordentlich A, Bromberg A, Kronman C, Marcus D, Lazar A, Ariel N, Velam B, Shafferman A. Allosteric modulation of acetylcholinesterase activity by peripheral ligands involves a conformational transition of the anionic subsite. Biochemistry 1995;34:15444–15452. [PubMed: 7492545]

Bourne Y, Taylor P, Radić ZA, Marchot P. Structural insights into ligand interactions at the acetylcholinesterase peripheral anionic site. EMBO 2003;22:1–12.

Ellman GL, Courtney D, Valentino A, Featherstone RM. A new and rapid colorimetric determination of acetylcholinesterase activity. Biochem Pharmacol 1961;7:88–95. [PubMed: 13726518]

Golicnik MD, Fournier D, Stojan J. Acceleration of *Drosophila* melangaster acetylcholinesterase methanesulfonyulation: peripheral ligand D-tubocurarine enhances the affinity for small methanesulfonylfluoride. Chem Biol Interact 2002;139:145–157. [PubMed: 11823003]

Gray PJ, Duggleby RG. Analysis of kinetic data for irreversible enzyme inhibition. Biochem J 1989;257 (2):419–424. [PubMed: 2930459]

Hart GJ, O'Brien RD. Recording spectrophotometric method for determination of dissociation and phosphorylation constants for the inhibition of acetylcholinesterase by organophosphates in the presence of substrate. Biochemistry 1973;12(15):2940–2945. [PubMed: 4737014]

Johnson JL, Cusack B, Davies MP, Fauq A, Rosenberry TL. Unmasking tandem site interaction in human acetylcholinesterase. Substrate activation with cationic acetanilide substrate. Biochemistry 2003;42:5438–5452. [PubMed: 12731886]

Kardos SA, Sultatos LG. Interactions of the organophosphates paraoxon and methyl paraoxon with mouse brain acetylcholinesterase. Toxicol Sci 2000;58:118–126. [PubMed: 11053548]

Kousba SA, Sultatos LG, Poet TS, Timchalk C. Comparison of chlorpyrifos-oxon and paraoxon acetylcholinesterase inhibition dynamics: Potential role of a peripheral binding site. Toxicol Sci 2004;80:239–248. [PubMed: 15141101]

Lin W, Tsou CL. Determination of rate constants for the irreversible inhibition of acetylcholine esterase by continuously monitoring the substrate reaction in the presence of the inhibitor. Biochim Biophys Acta 1986;870:185–190. [PubMed: 3955054]

Main AR. Affinity and phosphorylation constants for the inhibition of esterases by organophosphates. Sci 1964;144:992–993.

Mallender WD, Szegletes T, Rosenberry TL. Acetylthiocholine binds to Asp74 at the peripheral site of human acetylcholinesterase as the first step in the catalytic pathway. Biochemistry 2000;39(26): 7753–7763. [PubMed: 10869180]

Marcel VS, Estrada-Mondaca S, Magne F, Stojan J, Klaebe A, Fournier D. Exploration of the *Drosophila* acetylcholinesterase substrate activation site using a reversible inhibitor (Triton X-100) and mutated enzymes. J Biol Chem 2000;275:11603–11609. [PubMed: 10766776]

Masson HJ, Sains C, Stevenson AJ, Rawbone R. Rates of spontaneous reactivation and aging of acetylcholinesterase in human erythrocytes after inhibition by organophosphorus pesticides. Hum Exp Toxicol 2000;19:511–516. [PubMed: 11204553]

Mileson BE, Chambers JE, Chen WL, Dettburn W, Ehrich M, Eldefrawi AT, Gaylor DW, Hamernik K, Hodgson E, Karczmar AG, et al. Common mechanism of toxicity: A case study of organophosphorus pesticides. Toxicol Sci 1998;41:8–20. [PubMed: 9520337]

Radić Z, Pickering NA, Vellom DC, Camp S, Taylor P. Three distinct domains in the cholinesterase molecules confer selectivity for acetyl- and butyrylcholinesterase inhibitors. Biochemistry 1993;32:12074–12084. [PubMed: 8218285]

Radić Z, Taylor P. The influence of peripheral site ligands on the reaction of symmetric and chiral organophosphates with wildtype and mutant acetylcholinesterases. Chem Biol Interact 1999:119–120. 111–117. [PubMed: 10421445]

Radić Z, Taylor P. Peripheral site ligands accelerate inhibition of acetylcholinesterase by neutal organophosphates. J Appl Toxicol 2001;21:S13–S14. [PubMed: 11920914]

Rosenfeld C, Kousba A, Sultatos LG. Interactions of rat brain acetylcholinesterase with the detergent Trition X-100 and the organophosphate paraoxon. Toxicol Sci 2001;63:208–213. [PubMed: 11568364]

Rosenfeld CA, Sultatos LG. Concentration-dependent kinetics of acetylcholinesterase inhibition by the organophosphate paraoxon. Toxicol Sci 2006;90(2):460–469. [PubMed: 16403852]

Stojan J, Marcel V, Estrada-Mondaca S, Klaebe A, Masson P, Fournier D. A putative kinetic model for substrate metabolisation by *Drosophila* acetylcholinesterase. FEBS Let 1998;440:85–88. [PubMed: 9862431]

Sussman JL, Harel M, Frolow F, Oefner C, Goldman A, Toker L, Silman I. Atomic structure of acetylcholinesterase from *Torpedo californica*: A prototypic acetylcholine-binding protein. Science 1991;253:872–879. [PubMed: 1678899]

Szegletes T, Mallender WD, Thomas PJ, Rosenberry TL. Substrate binding to the peripheral site of acetylcholinesterase initiates enzymatic catalysis. Substrate inhibition arises as a secondary effect. Biochemistry 1999;38:122–133. [PubMed: 9890890]

Taylor P, Radić Z. The cholinesterases: From genes to proteins. Annu Rev Pharmacol Toxicol 1994;34:281–320. [PubMed: 8042853]

Timchalk C, Nolan RJ, Mendrala AL, Dittenber DA, Brzak KA, Mattsson JL. A physiologically based pharmacokinetic and pharmacodynamic (PBPK/PD) model for the organophosphate insecticide chlorpyrifos in rats and humans. Toxicol Sci 2002;66(1):34–53. [PubMed: 11861971]

Van Der Kloot W, Molgó J. Quantal acetylcholine release at the vertebrate neuromuscular junction. Physiol Rev 1994;74:899–991. [PubMed: 7938228]

Worek F, Diepold C, Eyer P. Dimethylphosphoryl-inhibited human cholinesterases: Inhibition, reactivation, and aging kinetics. Arch Toxicol 1999;73:7–14. [PubMed: 10207609]
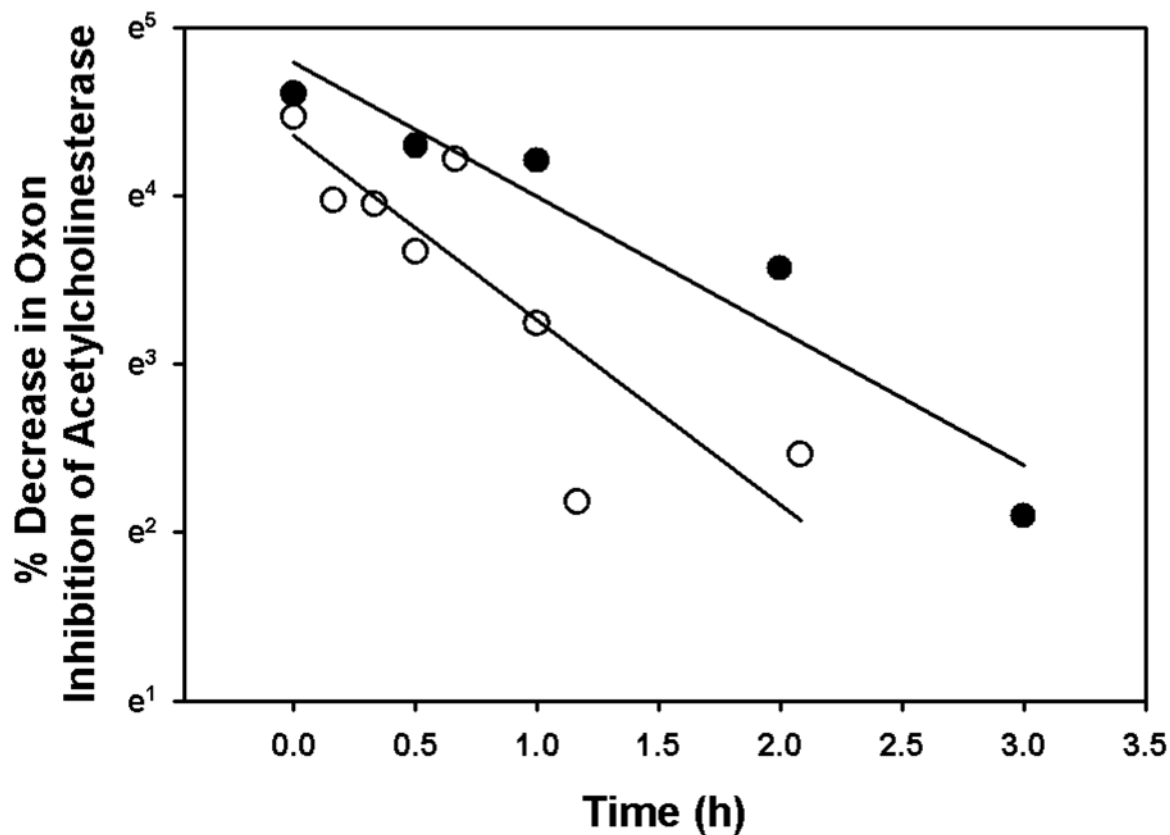
Figure 1.
Kinetic schemes descriptive of the interactions of acetylthiocholine, acetylcholine, or organophosphorus insecticide oxons with acetylcholinesterase. In this scheme, E represents free acetylcholinesterase, while AB represents substrate or inhibitor. Ligand bound to a secondary site is indicated by AB–E, whereas the Michaelis complex is denoted by E-AB. EA represents acetylated or phosphorylated enzyme, and B depicts the leaving groups. EA$_{aged}$ designates aged, enzyme-inhibitor complex. The pathway in bold depicts the simplest kinetic scheme, utilized by Main (1964), where binding only occurs at the active site. Aging and reactivation are often ignored when k_3 and k_4 are small. The k_i represents k_2/K_d under pseudo first order conditions (Main, 1964). The additional, non-bold pathways show a much more complex kinetic scheme that includes reversible binding to a secondary site. In the case of acetylthiocholine (and acetylcholine) this secondary site is the peripheral anionic site. In the case of organophosphates no such secondary site has been identified, but is suggested on the basis of kinetic data.

Figure 2.
Spontaneous decomposition of chlorpyrifos oxon (filled circles) and methyl paraoxon (open circles) in the absence of enzyme at 37°. The levels of oxon within incubations were evaluated by measuring the capacity of a sample of the incubation to inhibit 75–80 pM acetylcholinesterase by the Ellman reaction (Ellman *et al*, 1961). The slopes represent first order rate constants that are added to the k_i model to account for loss of each oxon as a result of spontaneous breakdown. This first order rate constant for chlorpyrifos oxon was 0.7967 h^{-1}, while that for methyl paraoxon was 1.0975 h^{-1}.
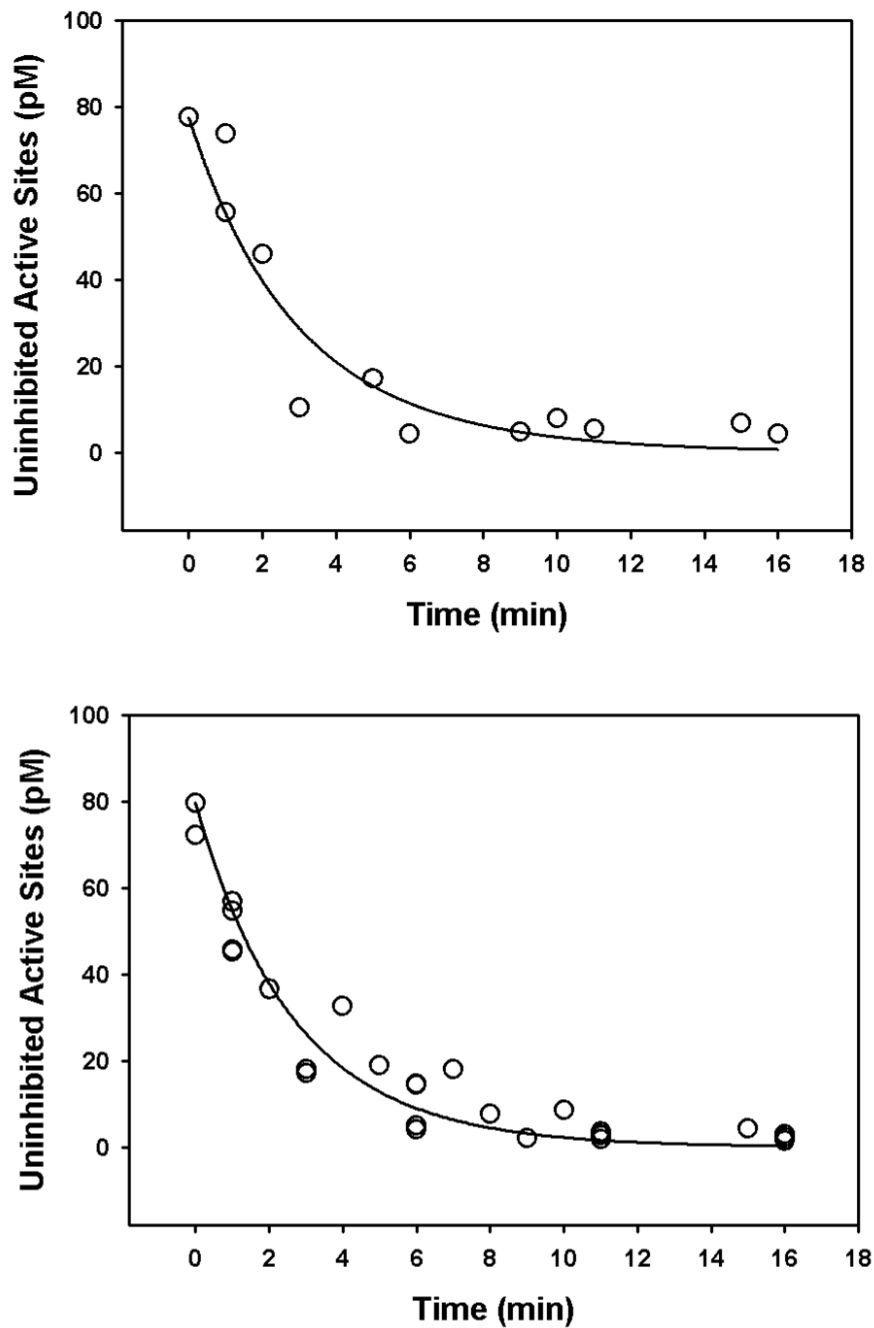
Figure 3.
Representative examples of k_i determinations with the k_i model. The upper panel shows a k_i determination for 2.5 nM methyl paraoxon at 37°, while the lower panel shows the k_i determination for 2.5 nM chlorpyrifos oxon at 24°. The open circles represent the empirical data while the solid lines represent the best-fit for the k_i model. The k_i for methyl paraoxon was found to be 8.24 nM^{-1} h^{-1}, whereas the k_i for chlorpyrifos oxon was 9.08 nM^{-1} h^{-1}.
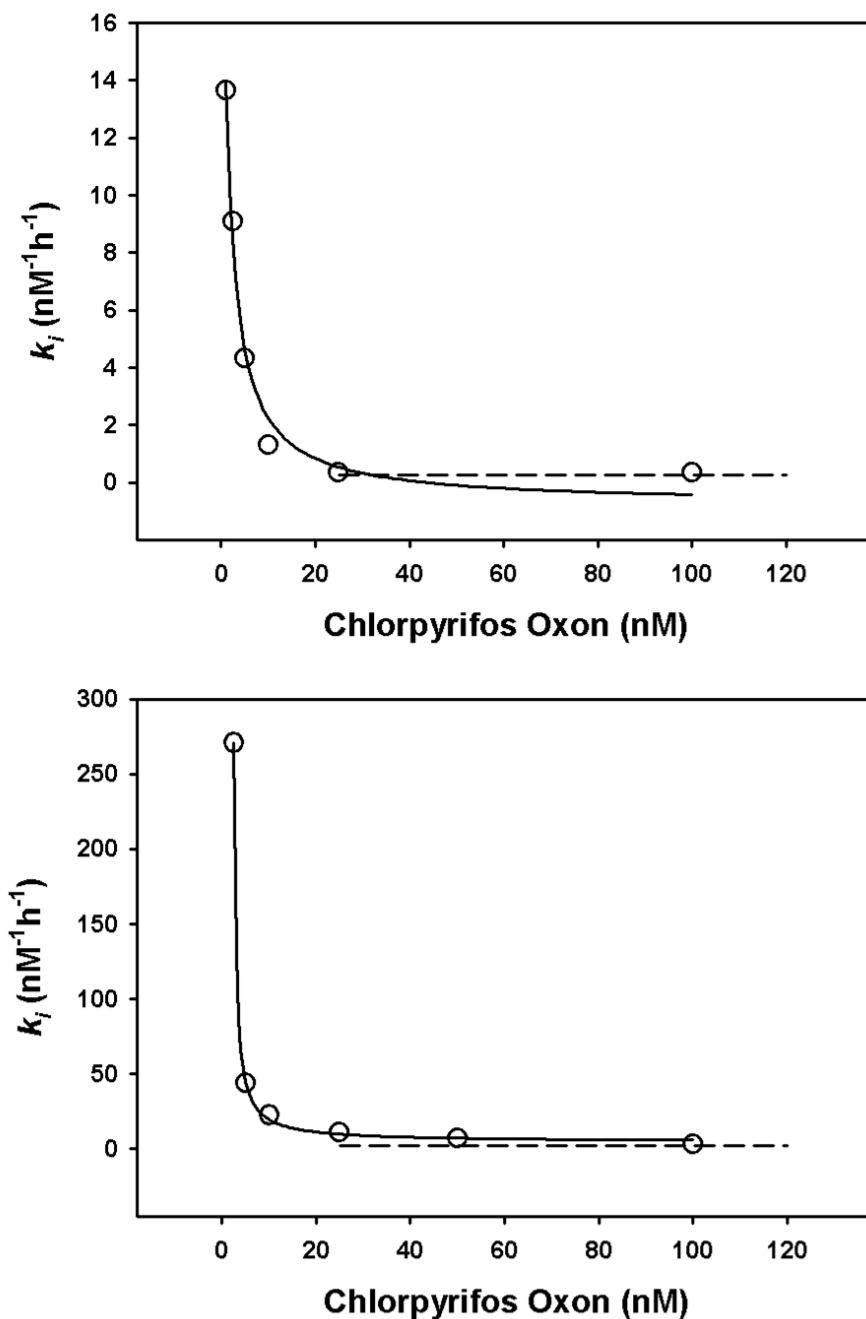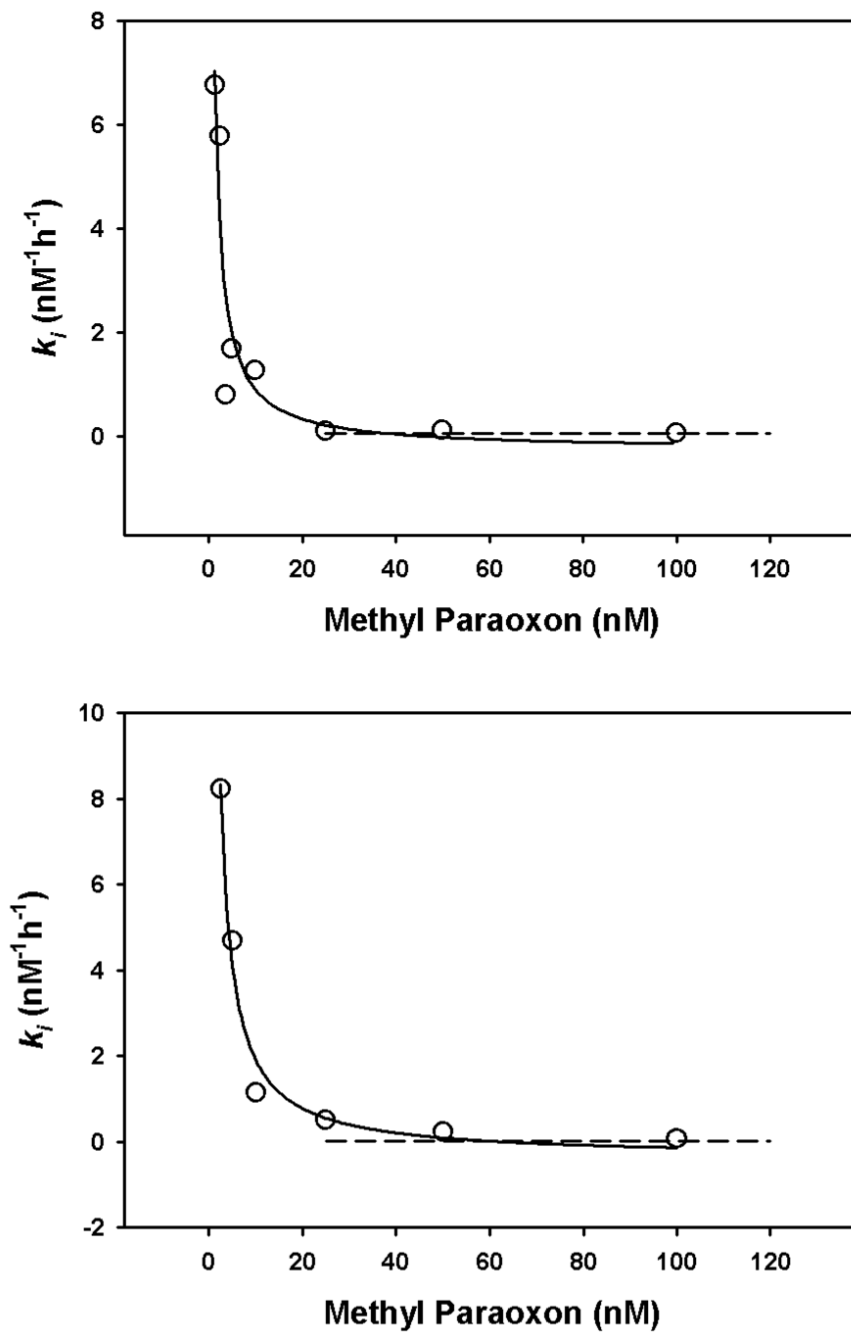
Figure 4.
Relationship of k_i and chlorpyrifos oxon concentration at 24° (upper panel, and 37° (lower panel). Each open circles depicts a k_i determined from inhibition profiles containing at least 10 data points (such as in Figures 4), and the solid line is the best-fit line from the equation y=a/(x+b)+c. At 24°, a=33.97, b=1.13, and c=0.74, whereas at 37° a=118.81, b=2.05, and c=4.48. The dashed lines depict the k_is determined by the traditional method of Main (1964), utilizing oxon concentrations greater than 20 nM.
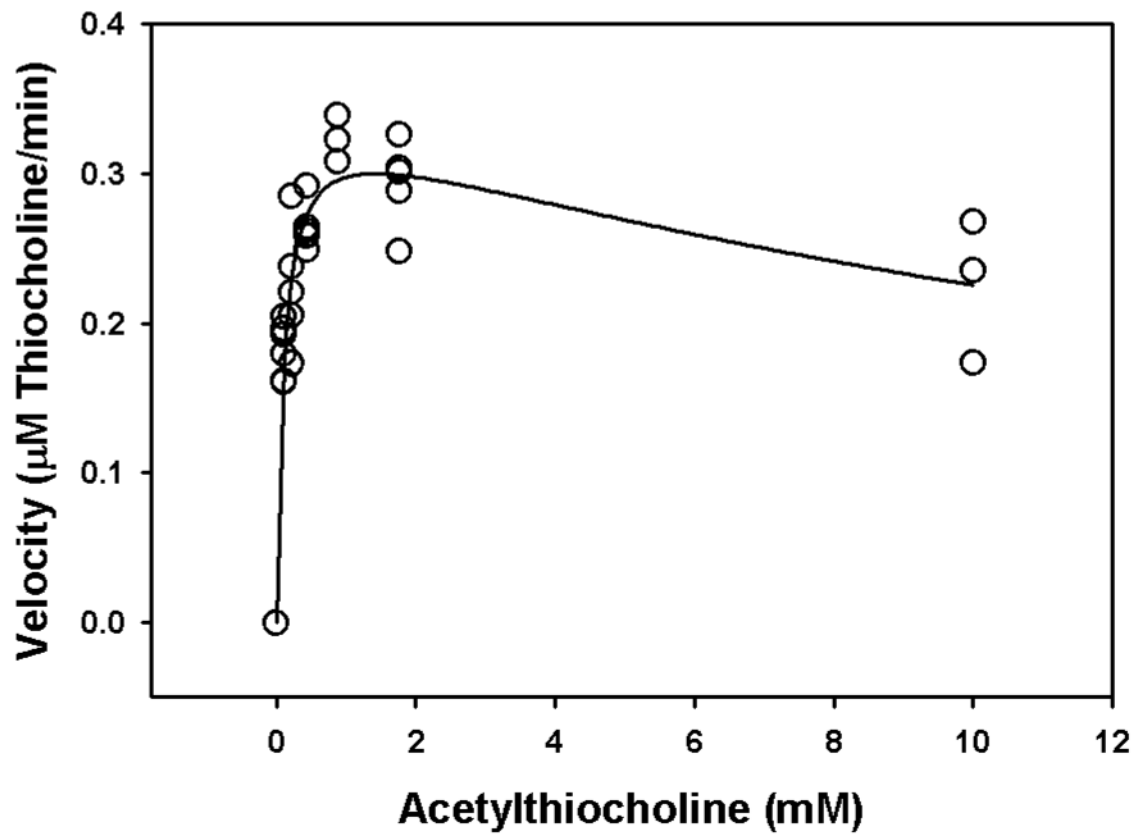
Figure 5.
Relationship of k_i and methyl paraoxon concentration at 24° (upper panel, and 37° (lower panel). Each open circles depicts a k_i determined from inhibition profiles containing at least 10 data points (such as in Figures 4), and the solid line is the best-fit line from the equation y=a/(x+b)+c. At 24°, a=23.17, b=0.16, and c=−0.3651, whereas at 37° a=33.97, b=1.13, and c=0.74. The dashed lines depict the k_is determined by the traditional method of Main (1964), utilizing oxon concentrations greater than 20 nM.

Figure 6.
Determination of the K_m for hydrolysis of acetylthiocholine by acetylcholinesterase. Each open circle is a single observation, whereas the solid line represents the best-fit of the Haldane equation (Radić *et al*, 1993). The $K_m = 0.1044$ mM, Vmax = 0.3440 mM/min, and $K_{ss} = 19.4820$ mM.
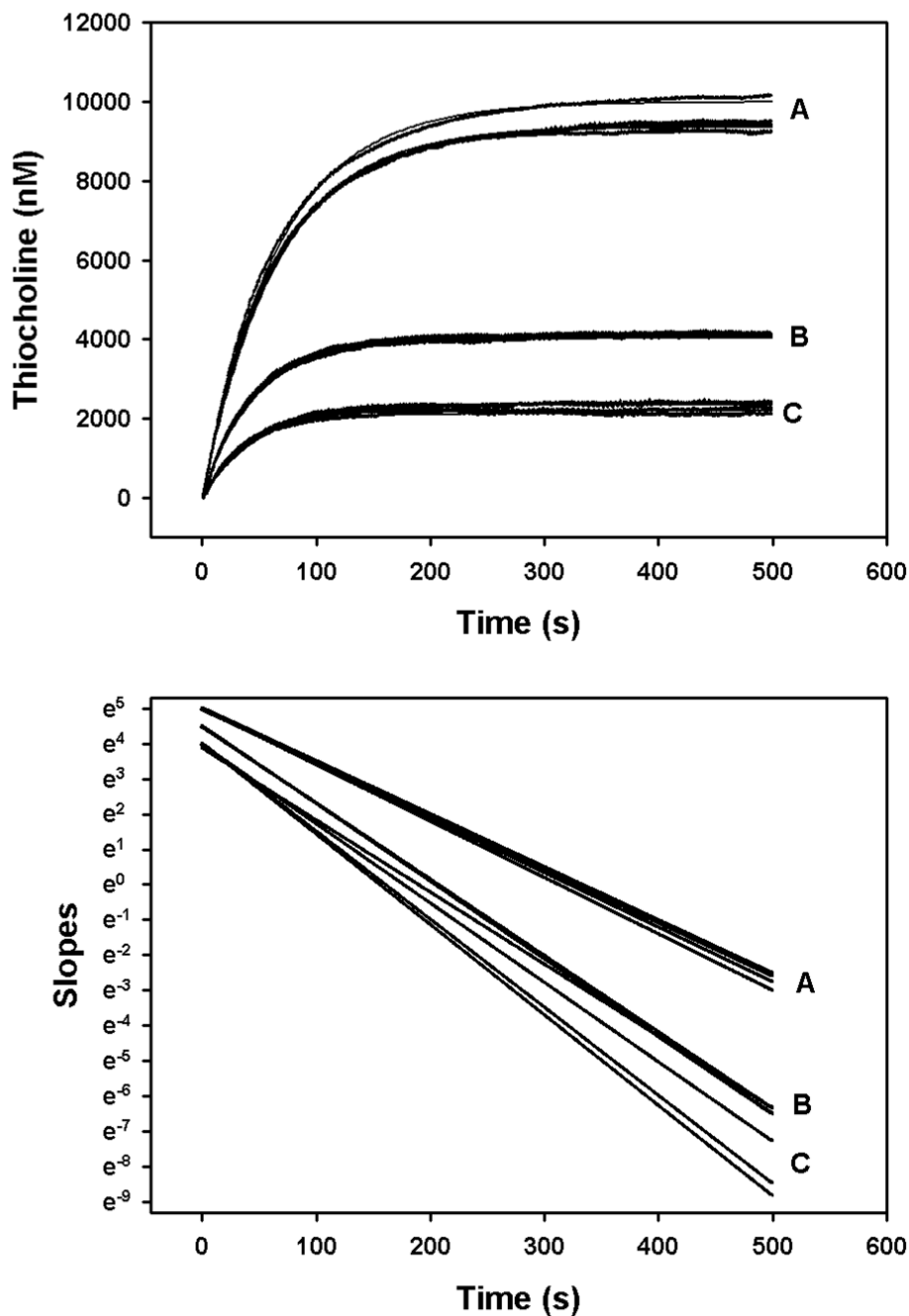
Figure 7.
Primary plot (upper panel) and secondary plot (lower panel) for determination of K_d and k_2 for 100 nM chlorpyrifos oxon by the zero-time method at 24°. The filled circles in the upper panel show the data generated by the stopped flow spectrophotometer, and the solid lines are the best-fit line as described under "Methods". The acetylcholinesterase active site concentrations ranged from 13 – 15 pM within the mixing chamber. The concentrations of acetylthiocholine used were: 0.055 mM (designated as A); 0.0275 mM (designated as B); and 0.01375 mM (designated as C). The lines in the lower panel are the slopes of the fitted lines from the upper panel, determined by analysis with cubic splines (Barak *et al*, 1995). The slopes and intercepts

of the lines in the lower panel were determined by linear regression analyses, and were used in Equations 8 and 10 to calculate K_d and k_2.
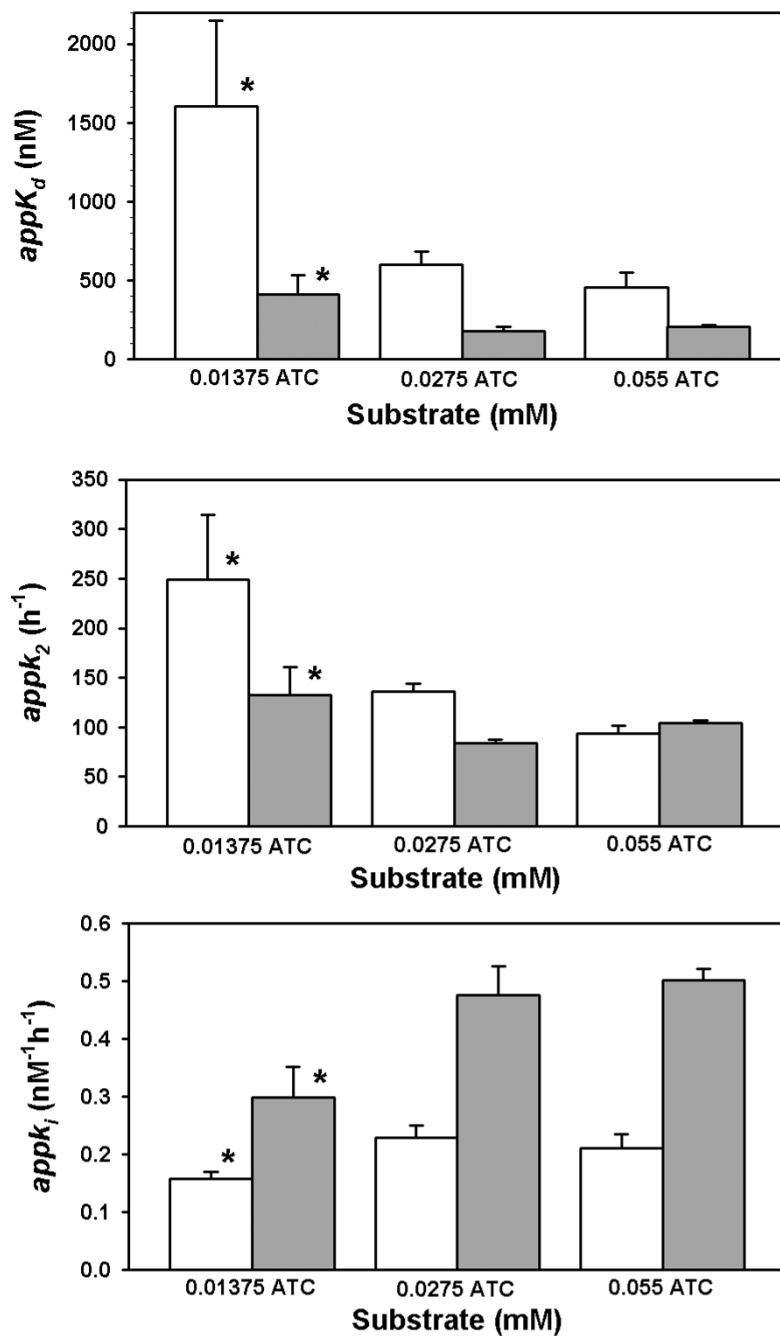
Figure 8.
Relationship between acetylthiocholine concentration and $appk_2$, $appK_d$, and $appk_i$ for 100 nM chlorpyrifos oxon at 24° (open bars) and 37° (filled bars). Each bar represents the mean ± standard deviation of at least three determinations as described in Figure 7. In the upper and middle panels, the asterisk indicates a significant difference ($p<0.05$) from the other groups at the same temperature by a Kruskal-Wallis one way analysis of variance on ranks, followed by multiple comparisons with Dunn's Method. In the lower panel the asterisk indicates a significant difference ($p<0.05$) from the other two groups at the same temperature by a one way analysis of variance followed by multiple comparisons with the Student-Newman-Keuls method.
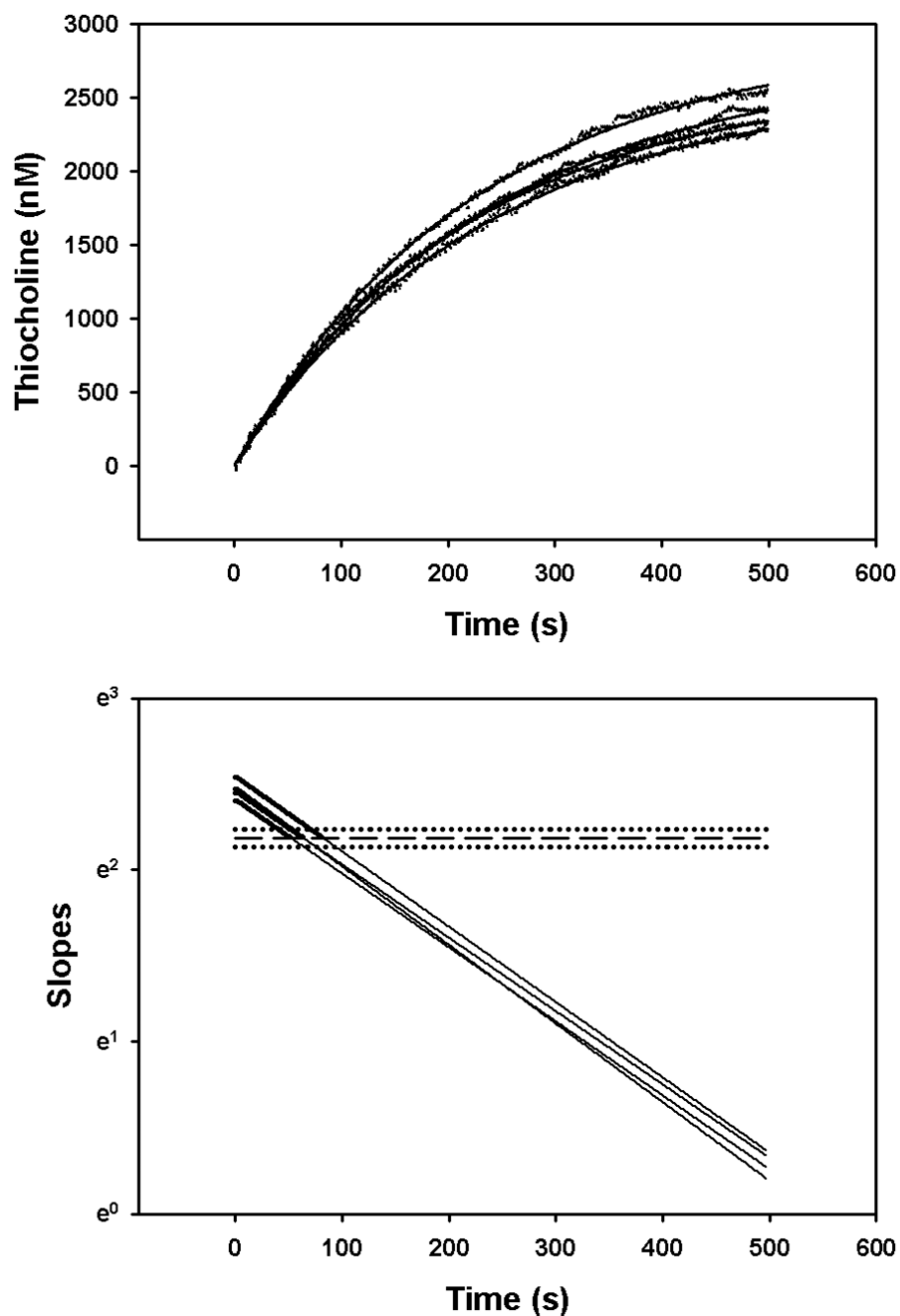
Figure 9.
Determination of initial velocities of 0.0275 mM acetylthiocholine hydrolysis in the presence of 10 nM chlorpyrifos oxon. The upper panel shows the empirical data (filled circles) fitted by equation (9) (solid lines). The acetylcholinesterase active site concentrations were 0.9 – 1 pM in the mixing chamber of the stopped flow spectrophotometer. The solid lines in the lower panel show the slopes of the fitted curves from the upper panel. The slopes were determined as described in "Methods". The bold portions of the curves indicate velocities greater than control velocities (without chorlpyrifos oxon). The control velocity mean (designated by the dashed line in the lower panel) and standard deviation (designated as the dotted lines) for an n=4 was 8.9059 ± 0.4813 nM/s.
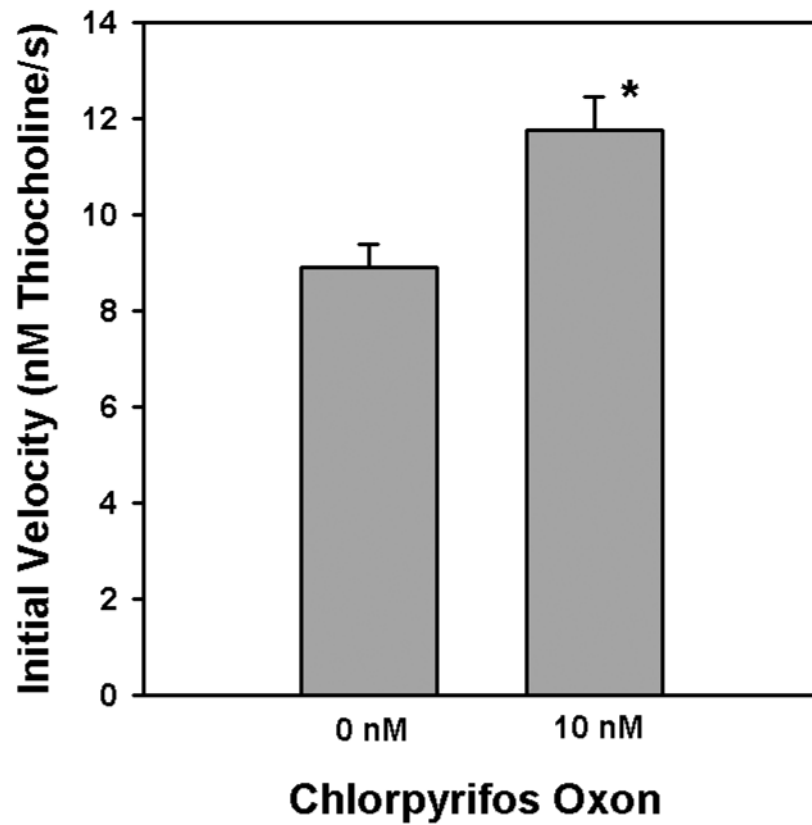
Figure 10.
Comparison of initial velocities of 0.0275 mM acetylthiocholine hydrolysis by
acetylcholinesterase in the presence and absence of 10 nM chlorpyrifos oxon. The initial
velocities were obtained by stopped-flow spectrophotometry, as described in "Methods". The
asterisk indicates a significant difference ($p<0.05$) from controls by a t-test.